Science Advances

AAAS

advances.sciencemag.org/cgi/content/full/4/1/eaao1054/DC1

Supplementary Materials for

Late formation of silicon carbide in type II supernovae

Nan Liu, Larry R. Nittler, Conel M. O'D. Alexander, Jianhua Wang

Published 17 January 2018, *Sci. Adv.* **4**, eaao1054 (2018)
DOI: 10.1126/sciadv.aao1054

This PDF file includes:

- Supplementary Text
- fig. S1. Silicon three-isotope plot comparing 62 X grains found on the three gold mounts to the 20 X grains and two ungrouped grains chosen for Ti-V isotope analysis in this study.
- fig. S2. R^2 for the correlation between the δ^{49}Ti* and δ^{30}Si values of X grains versus the ^{49}Ti/^{50}Ti production ratios in the He/C zone showing that the smaller the production ratio, the lower the R^2 value.
- fig. S3. The same as Fig. 3 but with δ^{49}Ti* calculated by adopting a ^{49}Ti/^{50}Ti production ratio of 0.50 instead of 1.04.
- fig. S4. δ^{49}Ti (upper panel) and ^{51}V/^{48}Ti (lower panel) versus NanoSIMS analysis cycle showing the inclusion of a Ti- and V-rich subgrain (gray region) within X grain M1-A8-G138, which had enhanced V/Ti ratios but no concomitant increase in δ^{49}Ti within analytical uncertainties (~100‰), indicating incorporation of a negligible amount of live ^{49}V, that is, formation after the decay of the majority of live ^{49}V in the Si/S zone.
- table S1. Carbon, N, Si, Al, K-Ca, and Ca-Ti isotopic compositions of two ungrouped SiC grains and one ungrouped graphite, KE3d-9 (*38*), separated from Murchison.

Supplementary Text

Assessment of the correlation between $\delta^{49}Ti$ and $\delta^{30}Si$ of X grains

Once we subtract the amount of ^{49}Ti from the He/C zone from the total ^{49}Ti budget of each X grain by adopting a $^{49}Ti/^{50}Ti$ production ratio of 1.04 for the He/C zone, the mean square of the weighted deviate (MSWD) value reduces from 26 (Fig. 2B) to 7.8 (Fig. 3) according to the *Isoplot* 4.15 geochronological toolkit (*40*), demonstrating the robustness of our approach. The MSWD value in Fig. 2B is 26, far from being perfect (MSWD=1), partly because of the variable contributions from the He/C zone to the ^{49}Ti budgets of the X grains, as shown in Fig. 3 in which the MSWD value reduces to 7.8. The rest of the grain data scatter in Fig. 3 (MSWD = 7.8) could be attributed to (1) variations in the isotopic and elemental compositions of the He/C zone, and (2) incorporation of different amounts of live ^{49}V relative to ^{48}Ti in individual grains due to V-Ti fractionation to varying degrees. The former could indicate (1) condensation of TiC grains prior to zonal mixing (i.e., Ti-Si fractionation within the Si/S and He/C zone) and mixing with material from more external layers of the He/C zone (*25*), thus resulting in variable elemental and isotopic compositions for the He/C zone relative to the Si/S zone even if the grains came from a single SN or (2) multiple SN stellar sources of X grains with varying elemental and isotopic compositions in their He/C zones.

Uncertainties in the $^{49}Ti/^{50}Ti$ production ratio in He/C zone

The total ^{49}Ti budget of each X grain includes contributions from ^{49}V decay in the Si/S zone and ^{49}Ti made by the neutron capture process in the He/C zone. Thus, it is necessary to subtract the amount of ^{49}Ti from the He/C zone in order to accurately estimate the contribution of ^{49}V decay. Given that ^{50}Ti in each X grain is essentially all from the He/C zone because ^{50}Ti is not made in the Si/S zone, we can thus reliably estimate the amount of ^{49}Ti from the He/C zone if the $^{49}Ti/^{50}Ti$ production ratio in the He/C zone is known. The production ratio can be inferred from the Ti isotopic compositions of three ungrouped grains inferred to have originated in SN outer zones, and was found to be near the solar $^{49}Ti/^{50}Ti$ ratio (1.04). The subtraction of ^{49}Ti from the He/C zone by adopting this number also significantly improves the correlation between $\delta^{49}Ti^*$ and $\delta^{30}Si$ values of X grains as can be seen by comparing Fig. 3 with Fig. 2B.

We, however, cannot completely exclude the possibility that the three ungrouped SN grains came from SNe that had a different neutron-capture environment from those of X grains. We therefore discuss the effect of uncertainties in the $^{49}Ti/^{50}Ti$ production ratio on our constraints of the X grain formation timing. First of all, 1.04 should represent the upper limit of the production ratio because one end of the negative trend in Fig. 3 reaches −1000‰, the minimum for δ notation. Thus, adoption of a higher production ratio will result in physically unrealistic $\delta^{49}Ti^*$ values below −1000‰, and thus can be excluded. Smaller production ratios, however, are possible, despite the fact that the smaller the production ratio, the smaller the R^2 value for the correlation between $\delta^{49}Ti^*$ and $\delta^{30}Si$ (fig. S2). Nonetheless, the possibility of smaller production ratios can only increase the $\delta^{49}Ti^*$ values of X grains, and in turn, increase the $\delta^{49}Ti_{Si/S}$ value (Fig. 2B and fig. S3 in comparison to Fig. 3). Thus, the derived lower limit for the formation timescale of X grains is not affected at all by this uncertainty.

Note that detailed nucleosynthetic calculations have shown that in addition to material from the Si/S and He/C zones, materials from He/N and envelope might have also been incorporated into X grains (e.g., *25*). Although for simplicity, we only include the Si/S and He/C zones for discussion, in fact all the discussion throughout the paper holds true if we extend the He/C zone to more external SN layers, because the He/C and He/N zones, and the envelope are all enriched in ^{29}Si, ^{30}Si, ^{49}Ti and ^{50}Ti relative to the inner Si/S zone. In addition, the neutron-capture process in the He/C zone mainly converts light isotopes to heavy isotopes of an element by capturing neutrons. Thus, the elemental ratios considered in this study are more or less the same in the outer zones.

Derivation of $\delta^{49}Ti_{Si/S}$

In the Si/S zone, ^{28}Si is abundantly produced by the α-capture process and as a result, $\delta^{30}Si$ is nearly −1000‰. In addition, the production of ^{50}Ti is essentially zero, i.e., $\delta^{50}Ti_{Si/S}$ =−1000‰. Thus, according to Equation (S6), when $\delta^{30}Si$=−1000‰, $\delta^{50}Ti_X$=$\delta^{50}Ti_{Si/S}$ =−1000‰; in turn, $\delta^{49}Ti^*$ = $\delta^{49}Ti_X$=$\delta^{49}Ti_{Si/S}$, which means that by extrapolating the negative correlation in Fig. 3 to $\delta^{30}Si$=−1000‰, the corresponding $\delta^{49}Ti^*$ value represents the $\delta^{49}Ti_{Si/S}$ value at the time of grain formation. On the other hand, according to the definition of $\delta^{49}Ti^*$ in Equation (S5), we can see that the variable $\delta^{49}Ti^*$ values of X grains in Fig. 3 are mainly caused by the variable contributions from the He/C zone to the ^{48}Ti budgets of X grains. Thus, $\delta^{49}Ti^*$ represents a mixture between the Si/S and He/C zones. For $\delta^{30}Si$, ^{28}Si receives contributions from both the Si/S zone and the He/C zone, while ^{30}Si is mainly from the He/C zone. Consequently, the negative trend in Fig. 3 is caused by different mixing ratios between the inner and outer zones, which can be extrapolated to the Si/S end-member ($\delta^{30}Si=-1000$‰) but not to the He/C end-member, because for $\delta^{30}Si>\sim-200$‰, the amount of $^{49}Ti_{Si/S}$ becomes negligible compared to the sum of $^{48}Ti_{Si/S}$ and $^{48}Ti_{He/C}$ in Equation (S5), i.e., $\delta^{49}Ti^{*}=-1000$‰. Thus, no trend can be observed in Fig. 3 toward the He/C end-member.

$$\delta\left(\frac{^{49}Ti}{^{48}Ti}\right)_X = \left[\frac{\frac{^{49}Ti_{He/C}}{^{48}Ti_{Si/S}+^{48}Ti_{He/C}}}{\left(\frac{^{49}Ti}{^{48}Ti}\right)_\odot}-1\right]\times 1000+\left[\frac{\frac{^{49}Ti_{Si/S}}{^{48}Ti_{Si/S}+^{48}Ti_{He/C}}}{\left(\frac{^{49}Ti}{^{48}Ti}\right)_\odot}-1\right]\times 1000+1000(S1)$$

where $\left(\frac{^{49}Ti}{^{48}Ti}\right)_\odot$ represents the solar ratio for $\frac{^{49}Ti}{^{48}Ti}$, and $^{i}Ti_{He/C}$ and $^{i}Ti_{Si/S}$ with i denoting 48, 49 or 50 are the amounts of ^{i}Ti from He/C and Si/S zones, respectively.

By asussming that the production ratio for $\frac{^{49}Ti}{^{50}Ti}$ in the He/C zone equals to the solar ratio,

$$\frac{^{50}Ti_{He/C}}{\left(\frac{^{50}Ti}{^{48}Ti}\right)_\odot} = \frac{^{49}Ti_{He/C}}{\left(\frac{^{49}Ti}{^{48}Ti}\right)_\odot}(S2)$$

Since $^{50}Ti_{He/C} >> {^{50}Ti_{Si/S}}$, the $\delta\left(\frac{^{50}Ti}{^{48}Ti}\right)_X$ value for an X grain can be written as

$$\delta\left(\frac{^{50}Ti}{^{48}Ti}\right)_X = \left[\frac{\frac{^{50}Ti_{He/C}}{^{48}Ti_{Si/S}+^{48}Ti_{He/C}}}{\left(\frac{^{50}Ti}{^{48}Ti}\right)_\odot}-1\right]\times 1000$$

$$= \left[\frac{\frac{^{49}Ti_{He/C}}{^{48}Ti_{Si/S}+^{48}Ti_{He/C}}}{\left(\frac{^{49}Ti}{^{48}Ti}\right)_\odot}-1\right]\times 1000(S3)$$

By substituting Equation (S3) into Equation (S1), we obtain

$$\delta\left(\frac{^{49}Ti}{^{48}Ti}\right)_X = \delta\left(\frac{^{50}Ti}{^{48}Ti}\right)_X + \left[\frac{\frac{^{49}Ti_{Si/S}}{^{48}Ti_{Si/S}+^{48}Ti_{He/C}}}{\left(\frac{^{49}Ti}{^{48}Ti}\right)_\odot}-1\right]\times 1000+1000(S4)$$

We define

$$\delta\left(\frac{^{49}Ti}{^{48}Ti}\right)^* = \left[\frac{\frac{^{49}Ti_{Si/S}}{^{48}Ti_{Si/S}+^{48}Ti_{He/C}}}{\left(\frac{^{49}Ti}{^{48}Ti}\right)_\odot}-1\right]\times 1000(S5)$$

By substituting Equation (S5) into Equation (S4), we obtain

$$\delta\left(\frac{^{49}Ti}{^{48}Ti}\right)^* = \delta\left(\frac{^{49}Ti}{^{48}Ti}\right)_X - \delta\left(\frac{^{50}Ti}{^{48}Ti}\right)_X - 1000(S6)$$

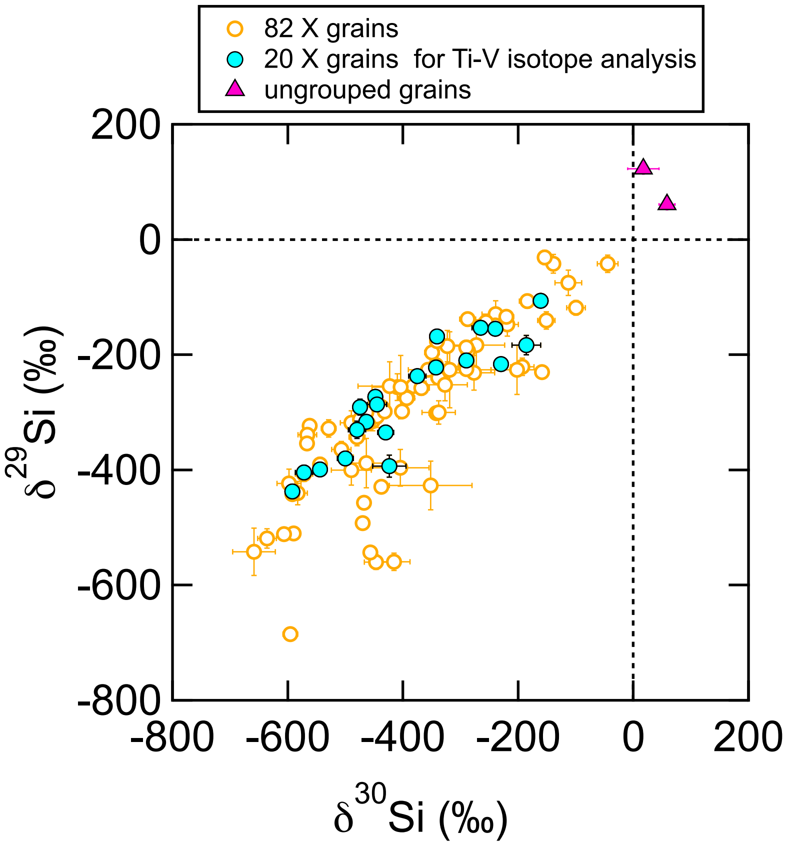

fig. S1. Silicon three-isotope plot comparing 62 X grains found on the three gold mounts to the 20 X grains and two ungrouped grains chosen for Ti-V isotope analysis in this study.

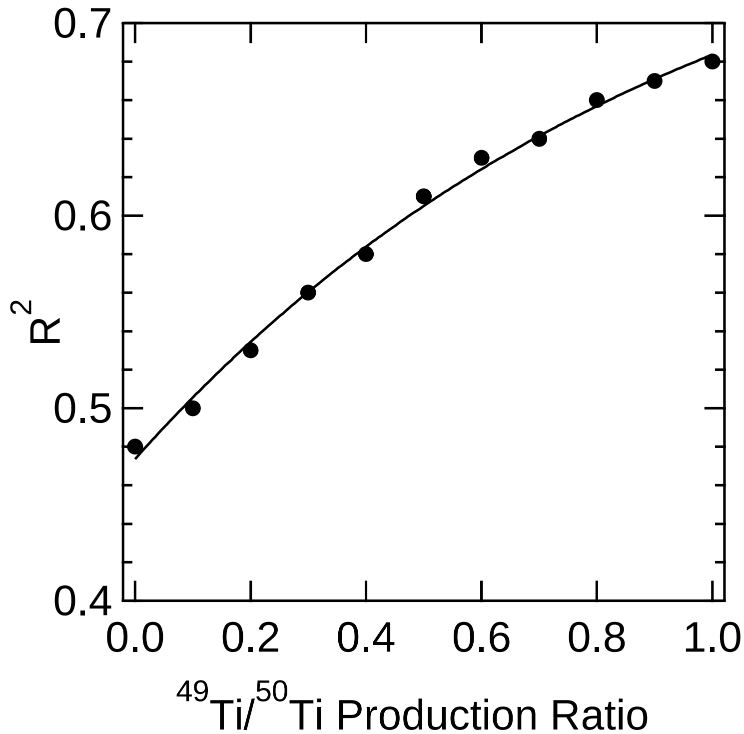

fig. S2. R^2 **for the correlation between the** δ^{49}**Ti* and** δ^{30}**Si values of X grains versus the** ^{49}**Ti/**^{50}**Ti production ratios in the He/C zone showing that the smaller the production ratio, the lower the** R^2 **value.**

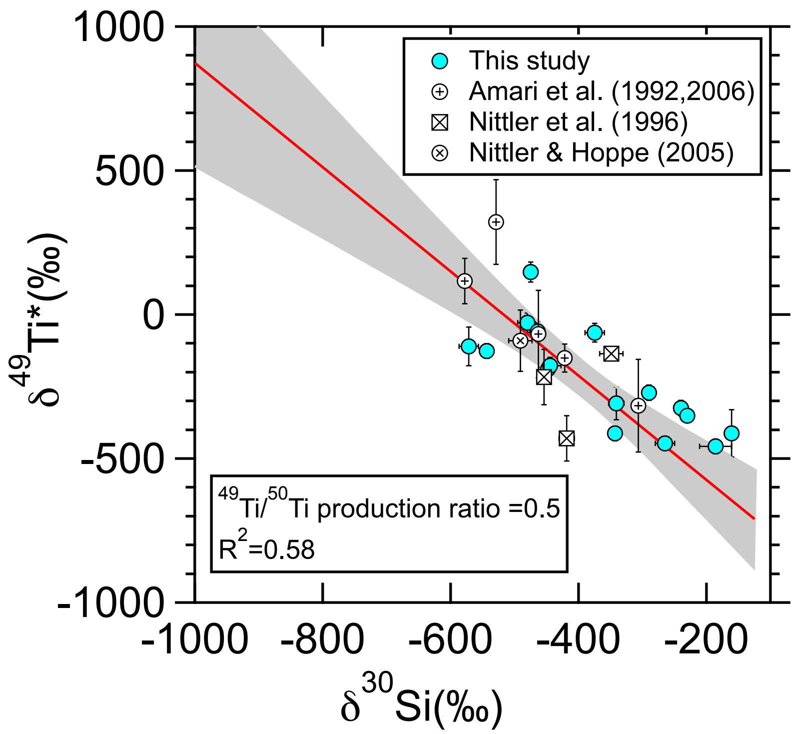

fig. S3. The same as Fig. 3 but with δ^{49}Ti* calculated by adopting a ^{49}Ti/^{50}Ti production ratio of 0.50 instead of 1.04. With this production ratio, the inferred $\delta^{49}Ti_{Si/S}$ at δ^{30}Si=−1000‰ is 879±358‰ and thus higher than the $\delta^{49}Ti_{Si/S}$ obtained by adopting 1.04 for the production ratio, 282±305‰. The fact that the maximal $\delta^{49}Ti_{Si/S}$ predicted by SN models is 500‰ implies that the ^{49}Ti/^{50}Ti production ratio lies above 0.5 but below 1.0 with limited variations.

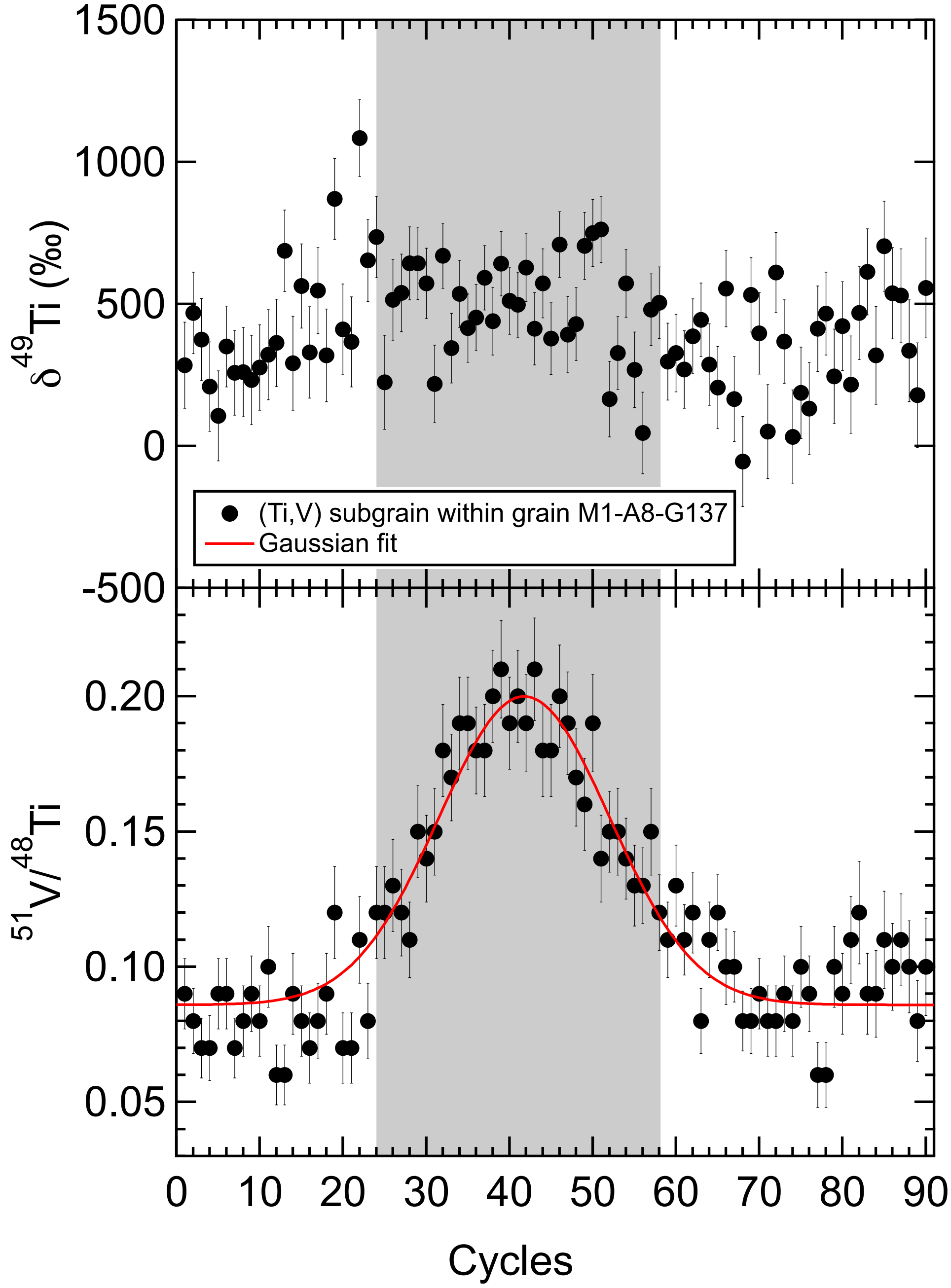

fig. S4. δ^{49}Ti (upper panel) and ^{51}V/^{48}Ti (lower panel) versus NanoSIMS analysis cycle showing the inclusion of a Ti- and V-rich subgrain (gray region) within X grain M1-A8-G138, which had enhanced V/Ti ratios but no concomitant increase in δ^{49}Ti within analytical uncertainties (~100‰), indicating incorporation of a negligible amount of live ^{49}V, that is, formation after the decay of the majority of live ^{49}V in the Si/S zone.

table S1. Carbon, N, Si, Al, K-Ca, and Ca-Ti isotopic compositions of two ungrouped SiC grains and one ungrouped graphite, KE3d-9 (*38*), separated from Murchison. Uncertainties are 1σ. The initial $^{41}Ca/^{40}Ca$ ratio of grain M1-A5-G676 is inferred from a $\delta^{41}K$ anomaly of 2670±235‰.

Grain	Size (μm)	Morphology	$^{12}C/^{13}C$	$^{14}N/^{15}N$	$^{16}O/^{18}O$	$\delta^{29}Si$	$\delta^{30}Si$
M1-A5-G676	1.4×1.4	S	139±1.4	17±0.3		61±9	58±14
M3-G1472	0.9×0.7	S	436±17	11±0.2		123±9	17±27
KE3d-9	8.0×8.0	Graphite	83±0.3		114±1.9	1272±75	937±66

Name	$^{26}Al/^{27}Al$ (×1000)	$^{41}Ca/^{40}Ca$	$\delta^{42}Ca$	$\delta^{43}Ca$	$\delta^{44}Ca$	$^{44}Ti/^{48}Ti$
M1-A5-G676	62±1.0	0.003±0.0001				
M3-G1472	17±0.4		63±117	−570±163	1980±128	0.75±0.01
KE3d-9	5.6±1.0		580±147	1799±382	894±109	

Name	$\delta^{46}Ti$	$\delta^{47}Ti$	$\delta^{49}Ti$	$\delta^{50}Ti$	V/Ti
M1-A5-G676	125±55	35±75	185±16	176±10	0.081
M3-G1472	83±71	209±78	1134±28	1052±18	0.160
KE3d-9	30±31	521±41	1717±77	1825±83	